

Weierstraß-Institut für Angewandte Analysis und Stochastik

im Forschungsverbund Berlin e.V.

Preprint

ISSN 0946 – 8633

Numerical Analysis of Monochromatic Surface Waves in a Poroelastic Medium

Bettina Albers

submitted: 28th July 2004

Weierstrass Institute
for Applied Analysis
and Stochastics
Mohrenstraße 39
10117 Berlin
Germany
E-Mail: albers@wias-berlin.de

No. 949

Berlin 2004



2000 *Mathematics Subject Classification.* 74J15, 76S05, 74S99.

Key words and phrases. Surface waves, flows in porous media, numerical analysis of dispersion relation.

Edited by
Weierstraß-Institut für Angewandte Analysis und Stochastik (WIAS)
Mohrenstraße 39
10117 Berlin
Germany

Fax: + 49 30 2044975
E-Mail: preprint@wias-berlin.de
World Wide Web: <http://www.wias-berlin.de/>

Abstract. The dispersion relation for surface waves on the boundary between a fully saturated poroelastic medium and a vacuum is investigated numerically in the whole range of frequencies. A linear model of a two-component poroelastic medium similar to but simpler than the classical Biot's model is used.

In the whole range of frequencies there exist two modes of surface waves corresponding to the classical Rayleigh and Stoneley waves. The numerical results for phase velocities, group velocities and attenuations of these waves are shown for different values of the bulk permeability coefficient, π .

1 Introduction

The most popular model for the study of surface waves in two-component porous media is the model of Biot [2]. One of the first investigations of surface waves within this model stems from Deresiewicz [4]. An extensive analysis of Biot's model in the range of high frequencies was carried by Feng & Johnson [7]. They show some basic properties of surface waves for the boundary porous medium/fluid (open and sealed boundary) in different ranges of the stiffness of the skeleton.

In this work we rely on a "simple mixture model" and this is, of course, simpler than that of Biot. We neglect two effects:

- an added mass effect reflected in the Biot's model by off-diagonal contributions to the matrix of partial mass densities,
- a static coupling effect between partial stresses.

The first contribution is neglected because it yields a non-objectivity of Biot's equations (see e.g. [9]). The second contribution is neglected because it yields small quantitative changes (app. 5%) [11] and does not influence spectral qualitative properties of surface waves.

The purpose of this work is to investigate the dispersion relation for surface waves on an impermeable boundary of a fully saturated poroelastic medium in the *whole range* of frequencies. Until now this has not been performed within the Biot's model because it yields a very complicated analysis of complex roots of the dispersion relation. Even though not straightforward either, it is simpler in the "simple mixture model".

2 Model

In this section we present the linear form of an extract of the "simple mixture model" of a two-component poroelastic saturated medium. (For the complete model see e.g. Wilmanski [8]).

The process is described by the *macroscopic* fields $\rho^F(\mathbf{x}, t)$ – partial mass density of the fluid, $\mathbf{v}^F(\mathbf{x}, t)$ – velocity of the fluid, $\mathbf{v}^S(\mathbf{x}, t)$ – velocity of the skeleton, $\mathbf{e}^S(\mathbf{x}, t)$ – symmetric tensor of small deformations of the skeleton. They satisfy the following relations

$$\begin{aligned} \frac{\partial \rho^F}{\partial t} + \rho_0^F \operatorname{div} \mathbf{v}^F &= 0, & \left| \frac{\rho^F - \rho_0^F}{\rho_0^F} \right| &\ll 1, \\ \rho_0^F \frac{\partial \mathbf{v}^F}{\partial t} + \kappa \operatorname{grad} \rho^F + \hat{\mathbf{p}} &= 0, & \hat{\mathbf{p}} &:= \pi (\mathbf{v}^F - \mathbf{v}^S), \\ \rho_0^S \frac{\partial \mathbf{v}^S}{\partial t} - \operatorname{div} (\lambda^S (\operatorname{tr} \mathbf{e}^S) \mathbf{1} + 2\mu \mathbf{e}^S) - \hat{\mathbf{p}} &= 0, \end{aligned} \tag{1}$$

$$\frac{\partial \mathbf{e}^S}{\partial t} = \text{sym grad } \mathbf{v}^S, \quad \|\mathbf{e}^S\| \ll 1.$$

Here ρ_0^F, ρ_0^S denote constant reference values of the partial mass densities, and $\kappa, \lambda^S, \mu^S, \pi$ are constant material parameters. The first one describes the macroscopic compressibility of the fluid component, the next two are macroscopic elastic constants of the skeleton and π is the coefficient of bulk permeability. We do not quote the equation for the porosity because the problem of evolution of porosity, which in this model is a field, can be solved separately from the rest of the problem and does not influence the propagation of acoustic waves in the medium.

2.1 Construction of solution

For the construction of solution we follow the procedure applied before in the works [10], [6] and [12]. We consider solely monochromatic waves with a given *real frequency* ω .

Compatibility with field equations We introduce the displacement vector \mathbf{u}^S for the skeleton, and formally the displacement vector \mathbf{u}^F for the fluid:

$$\begin{aligned} \mathbf{u}^S &= \text{grad } \varphi^S + \text{rot } \boldsymbol{\psi}^S, & \mathbf{v}^S &= \frac{\partial \mathbf{u}^S}{\partial t}, & \mathbf{e}^S &= \text{sym grad } \mathbf{u}^S, \\ \mathbf{u}^F &= \text{grad } \varphi^F + \text{rot } \boldsymbol{\psi}^F, & \mathbf{v}^F &= \frac{\partial \mathbf{u}^F}{\partial t}. \end{aligned} \quad (2)$$

For the two-dimensional case we make the following ansatz for monochromatic wave solutions in the x -direction

$$\begin{aligned} \varphi^S &= A^S(z) \exp[i(kx - \omega t)], & \varphi^F &= A^F(z) \exp[i(kx - \omega t)], \\ \psi_y^S &= B^S(z) \exp[i(kx - \omega t)], & \psi_y^F &= B^F(z) \exp[i(kx - \omega t)], \\ \psi_x^S &= \psi_z^S = \psi_x^F = \psi_z^F = 0, & \rho^F - \rho_0^F &= A_\rho^F(z) \exp[i(kx - \omega t)]. \end{aligned} \quad (3)$$

Substitution in field equations (1) leads to compatibility conditions

$$\begin{aligned} B^F &= \frac{i\pi}{\rho_0^F \omega + i\pi} B^S, & A_\rho^F &= -\rho_0^F \left(\frac{d^2}{dz^2} - k^2 \right) A^F, \\ \left[\kappa \left(\frac{d^2}{dz^2} - k^2 \right) + \omega^2 \right] A^F &+ \frac{i\pi}{\rho_0^F} \omega (A^F - A^S) = 0, \\ \left[\frac{\lambda^S + 2\mu^S}{\rho_0^S} \left(\frac{d^2}{dz^2} - k^2 \right) + \omega^2 \right] A^S &- \frac{i\pi}{\rho_0^S} \omega (A^F - A^S) = 0, \\ \left[\frac{\mu^S}{\rho_0^S} \left(\frac{d^2}{dz^2} - k^2 \right) + \omega^2 + \frac{i\pi \rho_0^F}{\rho_0^S (\rho_0^F \omega + i\pi)} \omega^2 \right] B^S &= 0. \end{aligned} \quad (4)$$

Dimensionless notation Introduction of a dimensionless notation is convenient. Using relations

$$c_{P1} := \sqrt{\frac{\lambda^S + 2\mu^S}{\rho_0^S}}, \quad c_{P2} := \sqrt{\kappa}, \quad c_S := \sqrt{\frac{\mu^S}{\rho_0^S}}. \quad (5)$$

which are the front velocities of the three bulk waves in a two-component porous medium: two longitudinal waves, $P1$ (fast wave) and $P2$ (slow wave, also called Biot's wave), and

one shear wave, S , we define the following dimensionless quantities

$$\begin{aligned} c_s &:= \frac{c_S}{c_{P1}} < 1, & c_f &:= \frac{c_{P2}}{c_{P1}}, & \pi' &:= \frac{\pi\tau}{\rho_0^S} > 0, \\ r &:= \frac{\rho_0^F}{\rho_0^S} < 1, & z' &:= \frac{z}{c_{P1}\tau}, & k' &:= kc_{P1}\tau, & \omega' &:= \omega\tau, \end{aligned} \quad (6)$$

where τ is the relaxation time (arbitrarily chosen for the purpose of this work).

Ansatz Further we omit the prime for typographical reasons. Substitution of (6) in equations (4) yields

$$\begin{aligned} \left[c_f^2 \left(\frac{d^2}{dz^2} - k^2 \right) + \omega^2 \right] A^F + i \frac{\pi}{r} \omega (A^F - A^S) &= 0, \\ \left[\left(\frac{d^2}{dz^2} - k^2 \right) + \omega^2 \right] A^S - i\pi\omega (A^F - A^S) &= 0, \\ \left[c_s^2 \left(\frac{d^2}{dz^2} - k^2 \right) + \omega^2 + \frac{i\pi\omega^2}{\omega + i\frac{\pi}{r}} \right] B^S &= 0. \end{aligned} \quad (7)$$

The matrix of coefficients for homogeneous materials is independent of z . Hence the differential eigenvalue problem can be easily solved. We seek solutions in the form

$$A^F = A_f^1 e^{\gamma_1 z} + A_f^2 e^{\gamma_2 z}, \quad A^S = A_s^1 e^{\gamma_1 z} + A_s^2 e^{\gamma_2 z}, \quad B^S = B_s e^{\zeta z}. \quad (8)$$

Substitution in (7) yields relations for the exponents in the form

$$\left(\frac{\zeta}{k} \right)^2 = 1 - \frac{1}{c_s^2} \left(1 + \frac{i\pi}{\omega + i\frac{\pi}{r}} \right) \left(\frac{\omega}{k} \right)^2, \quad (9)$$

$$\begin{aligned} c_f^2 \left[\left(\frac{\gamma}{k} \right)^2 - 1 \right]^2 + \left[1 + \left(1 + \frac{1}{r} \right) \frac{i\pi}{\omega} \right] \left(\frac{\omega}{k} \right)^4 \\ + \left[1 + c_f^2 + \left(c_f^2 + \frac{1}{r} \right) \frac{i\pi}{\omega} \right] \left[\left(\frac{\gamma}{k} \right)^2 - 1 \right] \left(\frac{\omega}{k} \right)^2 = 0. \end{aligned} \quad (10)$$

Simultaneously, we obtain for the eigenvectors the following relations

$$\mathbf{R}^1 = (B_s, A_s^1, A_f^1)^T, \quad \mathbf{R}^2 = (B_s, A_s^2, A_f^2)^T, \quad (11)$$

where

$$A_f^1 = \delta_f A_s^1, \quad A_s^2 = \delta_s A_f^2, \quad (12)$$

$$\delta_f := \frac{1}{r} \frac{\frac{i\pi}{\omega} \frac{\omega^2}{k^2}}{c_f^2 \left[\left(\frac{\gamma_1}{k} \right)^2 - 1 \right] + \left(\frac{\omega}{k} \right)^2 + \frac{i\pi}{\omega r} \frac{\omega^2}{k^2}}, \quad \delta_s := \frac{\frac{i\pi}{\omega} \frac{\omega^2}{k^2}}{\left(\frac{\gamma_2}{k} \right)^2 - 1 + \left(\frac{\omega}{k} \right)^2 + \frac{i\pi}{\omega} \frac{\omega^2}{k^2}}. \quad (13)$$

The above solution for the exponents still leaves three unknown constants B_s, A_f^2, A_s^1 which must be specified from boundary conditions.

Boundary conditions In order to determine surface waves in a saturated poroelastic medium we need conditions for $z = 0$. For the boundary porous medium/vacuum we have the following boundary conditions

$$\bullet \quad T_{13}|_{z=0} \equiv T_{13}^S|_{z=0} = c_S^2 \rho_0^S \left(\frac{\partial u_1^S}{\partial z} + \frac{\partial u_3^S}{\partial x} \right) \Big|_{z=0} = 0, \quad (14)$$

$$\begin{aligned} \bullet \quad T_{33}|_{z=0} &\equiv (T_{33}^S - p^F)|_{z=0} = \\ &= c_{P1}^2 \rho_0^S \left(\frac{\partial u_1^S}{\partial x} + \frac{\partial u_3^S}{\partial z} \right) - 2c_S^2 \rho_0^S \frac{\partial u_1^S}{\partial x} + \\ &\quad - c_{P2}^2 (\rho^F - \rho_0^F)|_{z=0} = 0, \end{aligned} \quad (15)$$

$$\bullet \quad \frac{\partial}{\partial t} (u_3^F - u_3^S) \Big|_{z=0} = 0, \quad (16)$$

where u_1^S, u_3^S are x -, and z -components of the displacement \mathbf{u}^S , respectively, and u_3^F is the z -component of the displacement \mathbf{u}^F .

The first two conditions describe the continuity of the full traction, $\mathbf{t} := (\mathbf{T}^S + \mathbf{T}^F) \mathbf{n}$, $\mathbf{n} = (0, 0, 1)^T$, on the boundary; the third condition is the continuity of the fluid mass flux.

These conditions follow for this boundary from the more general boundary conditions formulated by Deresiewicz & Skalak [5] for the boundary porous medium/fluid.

Dispersion relation Substitution of the above results in the boundary conditions (14)-(16) yields the following equations for the three unknown constants B_s, A_f^2 and A_s^1

$$\mathbf{A} \mathbf{X} = \mathbf{0}, \quad (17)$$

where

$$\mathbf{A} := \begin{pmatrix} \left(\frac{\zeta}{k}\right)^2 + 1 & 2i\frac{\gamma_2}{k} \delta_s & 2i\frac{\gamma_1}{k} \\ -2ic_s^2 \frac{\zeta}{k} & \left[\left(\frac{\gamma_2}{k}\right)^2 - 1 + 2c_s^2\right] \delta_s + \left(\frac{\gamma_1}{k}\right)^2 - 1 + 2c_s^2 + \\ & + rc_f^2 \left[\left(\frac{\gamma_2}{k}\right)^2 - 1\right] & + rc_f^2 \left[\left(\frac{\gamma_1}{k}\right)^2 - 1\right] \delta_f \\ i\frac{r\omega}{r\omega + i\pi} & -(\delta_s - 1) \frac{\gamma_2}{k} & (\delta_f - 1) \frac{\gamma_1}{k} \end{pmatrix}, \quad (18)$$

$$\mathbf{X} := (B_s, A_f^2, A_s^1)^T. \quad (19)$$

This homogeneous set yields the *dispersion relation*: $\det \mathbf{A} = 0$ determining the $\omega - k$ relation. We investigate the numerical solution of this equation.

3 Numerical procedure and parameters

The problem $\det \mathbf{A} = 0$ has been solved for the wave number, k . From the complex results for k we are able to determine the normalized velocities of the Rayleigh and Stoneley modes $c'_{Ra} = \frac{\omega}{\text{Re } k_1}$, $c'_{St} = \frac{\omega}{\text{Re } k_2}$, respectively, and the corresponding normalized attenuations $\text{Im } k_1$ for the Rayleigh wave and $\text{Im } k_2$ for the Stoneley wave.

The results have been obtained for the following numerical data

$$\begin{aligned}
 \beta &= 0, & c_{P1} &= 2500 \frac{\text{m}}{\text{s}}, & c_{P2} &= 1000 \frac{\text{m}}{\text{s}}, & c_S &= 1500 \frac{\text{m}}{\text{s}}, \\
 \rho_0^S &= 2500 \frac{\text{kg}}{\text{m}^3}, & \rho_0^F &= 250 \frac{\text{kg}}{\text{m}^3}, & c_s &= \frac{c_S}{c_{P1}} = 0.6, & c_f &= \frac{c_{P2}}{c_{P1}} = 0.4, \\
 r = \frac{\rho_0^F}{\rho_0^S} &= 0.1, & \pi &= \begin{cases} 10^7 \frac{\text{kg}}{\text{m}^3\text{s}} \\ \text{or variable} \end{cases}, & \tau &= 10^{-6} \text{ s}, & \pi' := \frac{\pi\tau}{\rho_0^S} &= \begin{cases} 0.004 \\ \text{or variable} \end{cases}.
 \end{aligned} \tag{20}$$

These data correspond approximately to, for instance, either marls or porous and saturated sandstones [3].

4 Numerical results

In the whole range of frequencies there exist two surface modes of propagation corresponding to the classical Rayleigh and Stoneley waves.

Results are shown for different values of the bulk permeability coefficient, π . This parameter describes the resistance of the porous medium against the flow of the fluid.

4.1 Velocities of Rayleigh and Stoneley waves

Fig. 1 shows the phase velocities of the Rayleigh (left) and Stoneley (right) waves normalized by the $P1$ -velocity (see: (6)) in dependence on the frequency. The velocities are given for different values of the bulk permeability parameter π . We see a range of frequencies from zero to the very large value of 100 MHz. On the left figure we indicate additionally the high and low frequency limits of the Rayleigh wave common for all values of permeability. We see that, indeed, the results for intermediate frequencies lie between these limits.

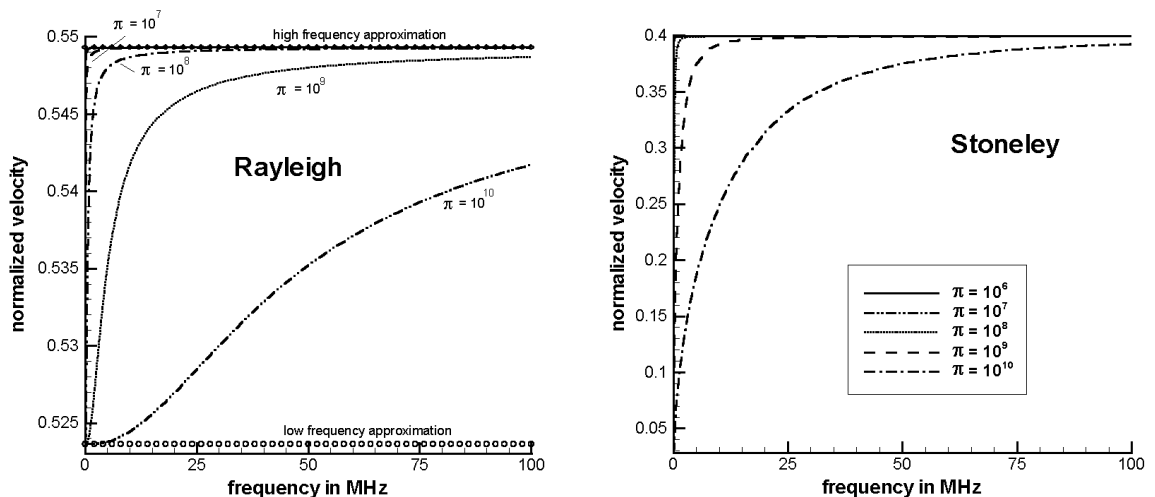


Fig. 1. Normalized velocities of the Rayleigh wave $c'_{Ra} \equiv \frac{c_{Ra}}{c_{P1}}$ and of the Stoneley wave $c'_{St} \equiv \frac{c_{St}}{c_{P1}}$ for different values of the permeability coefficient π in units $\left[\frac{\text{kg}}{\text{m}^3\text{s}} \right]$

In the range of very small frequencies the Rayleigh velocity remains nearly constant. This range depends on the permeability and grows with growing π . In this region of frequencies there exists a little decay of this velocity (app. 0.025% of the difference of limit values for

$\omega = 0$ and $\omega \rightarrow \infty$). Due to its small size this effect is not visible in this figure. Bourbié *et al.* [3] prescribe this effect to an influence of the P2-wave. The minimum value remains constant for different values of π . This means that the decay is not driven by the diffusion.

Curves for different values of π are selfsimilar. This is due to the fact that π and ω are normalized by the characteristic time τ : $\omega' = \omega\tau$, $\pi' = \frac{\pi\tau}{\rho_0^S}$ and these are the only independent parameters which contain τ . In other words we could use $\frac{\rho_0^S}{\pi}$ as a time normalization parameter. Certainly, as in the classical case of Rayleigh waves in a single component elastic medium, all values lie below the normalized velocity of the shear wave $c_s \equiv \frac{c_s}{c_{P1}} = 0.6$.

The Stoneley velocity increases from the zero value for $\omega = 0$. The growth is faster than the growth of the Rayleigh velocity but the maximum value is smaller. It lies always below the normalized velocity of the fluid $c_f \equiv \frac{c_{P2}}{c_{P1}} = 0.4$. This happens for all values of π . The maximum value of the Stoneley velocity appearing for $\omega \rightarrow \infty$ is approximately 0.15% smaller than the velocity of the fluid. One should point out that – differently than often stated – the Stoneley velocity behaves regularly in the whole range of frequencies and it ceases to exist only for $\omega = 0$. In the vicinity of this point the Stoneley velocity possesses a similar feature to the P2-wave: it decays to zero as $\sqrt{\omega}$.

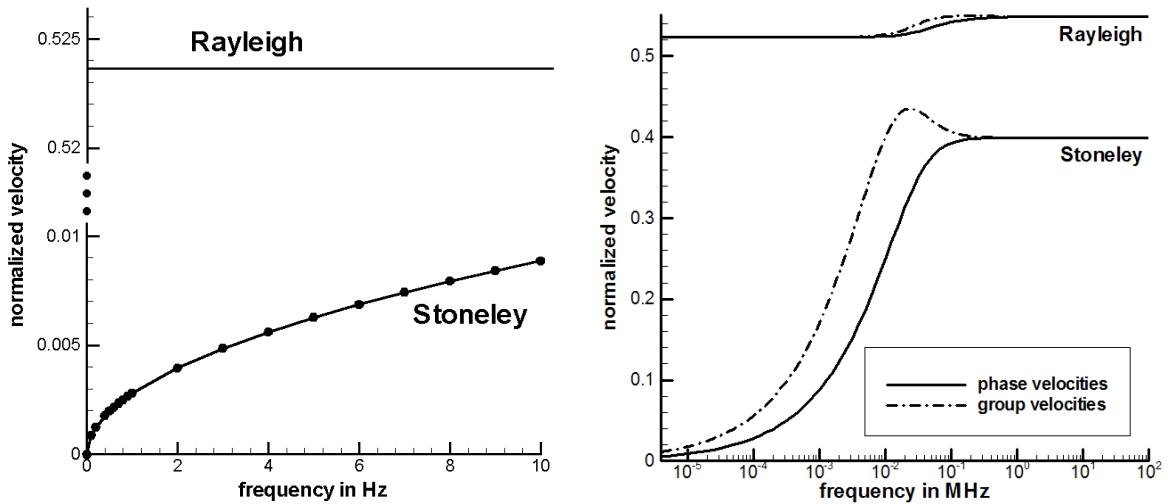


Fig. 2. Comparison of the behaviour of Rayleigh and Stoneley wave velocities for a permeability coefficient $\pi = 10^7 \frac{\text{kg}}{\text{m}^3\text{s}}$. Left: Phase velocities for low frequencies; right: phase and group velocities of both waves for a wide range of frequencies

In order to be more specific, in Fig. 2 we consider a selected case which may appear in geotechnics and show the normalized velocities of both Rayleigh and Stoneley waves for a permeability coefficient $\pi = 10^7 \frac{\text{kg}}{\text{m}^3\text{s}}$ and very low frequencies. This corresponds, as shown above, to sandstone saturated with water.

The figures for phase velocities of Rayleigh and Stoneley waves show that both of them depend on the frequency ω . This phenomenon is known as *dispersion*. In the present case dispersion is caused by diffusive dissipation (for $\pi = 0$ there is no dispersion). Monochromatic waves are an idealization which is never strictly realized in nature. Most sources emit signals with a continuous spectrum over a limited frequency band. The group velocity c_g (for details see e.g. [1]) for a given frequency ω is the velocity of transport of a wave package consisting of contributions from a band of frequencies around ω . In our case the

wave number k is complex. However, under the simplifying assumptions of a narrow band of frequencies, small changes of the amplitude and small changes of damping we are able to derive a similar relation for the group velocity to this for real wave numbers. We know that the wavenumber $k = k_R + ik_I$ and the phase velocity c_{ph} depend on the frequency. Then, with $k_R = \frac{\omega}{c_{ph}}$

$$\frac{dk_R}{d\omega} = \frac{1}{c_g} = \frac{1}{c_{ph}} - \frac{\omega}{c_{ph}^2} \frac{dc_{ph}}{d\omega}, \Rightarrow c_g = \frac{c_{ph}}{1 - \frac{\omega}{c_{ph}} \frac{dc_{ph}}{d\omega}}. \quad (21)$$

On the right hand side of Fig. 2 we show both the phase velocities and the group velocities of both surface waves. The derivative $\frac{dc_{ph}}{d\omega}$ has been calculated as central difference.

4.2 Attenuation of Rayleigh and Stoneley waves

This section is devoted to the behaviour of the attenuation of the Rayleigh and Stoneley waves. Imaginary parts of the wave number k determine the damping of waves. It is normalized by the product with the $P1$ -velocity and the relaxation time (see: (6)). This means for our parameters that the values presented in the figures are 400 times smaller than in real physical units.

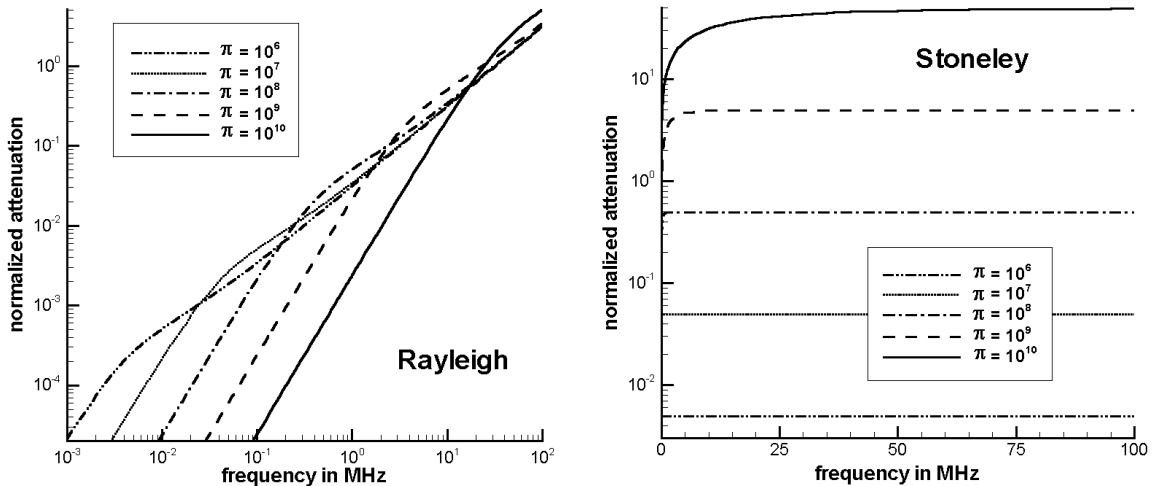


Fig. 3. Normalized attenuations of Rayleigh- and Stoneley waves for different values of the permeability coefficient π in units $\left[\frac{\text{kg}}{\text{m}^3\text{s}}\right]$.

Let us first turn our attention to the Rayleigh wave. Fig. 3 (left) shows the normalized attenuation of this wave. It is obvious that this wave is strongly attenuated. The attenuation linearly increases to infinity as $\omega \rightarrow \infty$. Similar to the attenuation of $P1$ -waves these curves intersect for different values of π . The impression that the attenuation would not start from zero with zero frequency stems from the double logarithmic plot of the curves. In reality the attenuation for all values of π starts from zero. The attenuation is in the same manner selfsimilar as the velocity.

Inspection of the right hand side of Fig. 3 shows that also the normalized attenuation of the Stoneley wave starts from the zero value for $\omega = 0$. But in contrast to the Rayleigh wave attenuation for small frequencies it increases much faster and then approaches a horizontal

asymptotic value for larger values of the frequency. This means the limit $\omega \rightarrow \infty$ is finite and dependent on the permeability coefficient π .

In order to expose a practically important region of very small frequencies, we present in Fig. 4 on the left hand side the attenuation of both surface waves and two bulk waves: $P1$ and $P2$ in the range of frequencies up to 1000 Hz. Clearly, in this range, the Rayleigh wave is attenuated stronger than the $P1$ wave but still weaker than $P2$. For low frequencies the attenuation of the Stoneley wave is much higher than this of the Rayleigh wave. Both attenuations are starting from zero for $\omega = 0$. The right hand side shows that the Stoneley wave attenuation increases rapidly until it reaches a certain value which depends on the permeability coefficient π , in the case under consideration – app. $0.0496 \times (c_{P1}\tau)^{-1} \simeq 19.84 \frac{1}{\text{m}}$. After reaching this value – which happens in the low frequency range – it remains almost constant. The Rayleigh wave attenuation, however, does not have a finite value for $\omega \rightarrow \infty$. In contrast to all other waves whose attenuation goes to a finite limit as $\omega \rightarrow \infty$ the attenuation of the Rayleigh wave grows unbounded. This is the feature of a *leaky wave*. Generally, the Rayleigh attenuation increases linearly with growing ω , only for very low frequencies the growth is a little bit faster. Consequently, there appears an intersection of the attenuation curves of both waves. This point lies in the range of high frequencies.

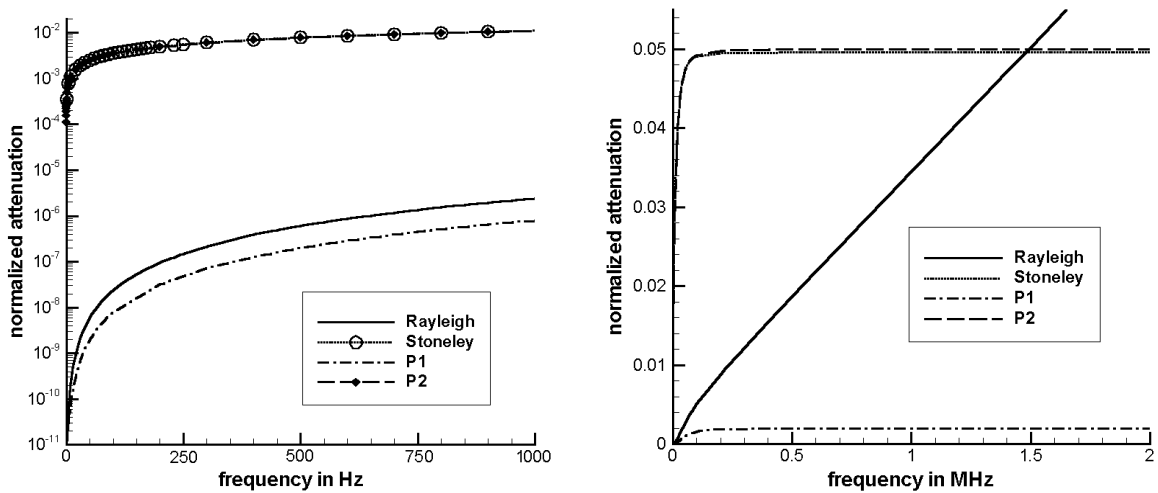


Fig. 4. Normalized attenuation of Rayleigh, Stoneley, $P1$ and $P2$ -wave, for $\pi = 10^7 \frac{\text{kg}}{\text{m}^3\text{s}}$ in different ranges of frequencies.

5 Concluding remarks

This work is devoted to the numerical investigation of the dispersion relation for surface waves on an impermeable boundary of a fully saturated poroelastic medium in the *whole range of frequencies*. In the whole range there exist two modes of surface waves corresponding to the classical Rayleigh and Stoneley waves. We have shown numerical results for the normalized velocities and attenuations of these waves for different values of the bulk permeability coefficient, π , in different ranges of frequencies, ω .

Rayleigh

- the velocity of propagation of this wave lies in the interval determined by the limits $\omega \rightarrow 0$ and $\omega \rightarrow \infty$. The high frequency limit is app. 4.7% higher than the low frequency limit. The velocity is always smaller than c_S , i.e. slower than the S -wave. As a function of ω it possesses an inflection point and it is slightly nonmonotonous,
- the attenuation of this wave grows from zero for $\omega = 0$ to infinity as $\omega \rightarrow \infty$. In the range of large frequencies it is linear. This means that it is a leaky wave.

Stoneley

- the velocity of this wave grows monotonically from the zero value for $\omega = 0$ to a finite limit which is slightly smaller (app. 0.15%) than the velocity c_{P2} of the $P2$ -wave. The growth of the velocity of this wave in the range of low frequencies is much steeper than this of Rayleigh waves
- both the velocity and attenuation of the Stoneley wave approach zero as $\sqrt{\omega}$,
- the attenuation of the Stoneley wave grows monotonically to a finite limit for $\omega \rightarrow \infty$. It is slightly smaller than the attenuation of $P2$ -waves. Consequently, in contrast to the claims in the literature, the Stoneley wave is attenuated.

Results for different values of the permeability coefficient π are selfsimilar, i.e. a change of π yields a corresponding change in the scale of the frequency axis for velocities, and of both axes for attenuations. Otherwise the qualitative behaviour remains unchanged.

References

1. A. Ben-Menahem, S. J. Singh: *Seismic waves and sources*, Dover (1981).
2. M. A. Biot: *Acoustics, elasticity and thermodynamics of porous media: Twenty-one papers by M. A. Biot*, I. Tolstoy (ed.), American Institute of Physics (1992).
3. T. Bourbié, O. Coussy, B. Zinszner: *Acoustics of porous media*, Editions Technip, Paris (1987).
4. H. Deresiewicz: The effect of boundaries on wave propagation in a liquid filled porous solid. IV. Surface waves in a half space, *Bull. Seismol. Soc. Am.*, **52**, 627-638 (1962).
5. H. Deresiewicz, R. Skalak: On uniqueness in dynamic poroelasticity, *Bull. Seismol. Soc. Am.*, **53**, 783-788 (1963).
6. I. Edelman, K. Wilmanski: Asymptotic analysis of surface waves at vacuum/porous medium and liquid/porous medium interfaces, *Cont. Mech. Thermodyn.*, 25-44, **14**, 1 (2002).
7. S. Feng, D.L. Johnson: High-frequency acoustic properties of a fluid/porous solid interface. I. New surface mode, *J. Acoust. Soc. Am.*, **74**(3), 906-914 (1983).
8. K. Wilmanski: Waves in porous and granular materials, in: *Kinetic and Continuum Theories of Granular and Porous Media*, K. Hutter, K. Wilmanski (eds.), 131-186, CISM Courses and Lectures No. 400, Springer Wien New York (1999).
9. K. Wilmanski: Some questions on material objectivity arising in models of porous materials, in: *Rational Continua, classical and new*, M. BROCATO (ed.), 149-161, Springer-Verlag, Italia Srl, Milano (2001).

10. K. Wilmanski: Propagation of sound and surface waves in porous materials, in: B. Maruszewski (ed.), *Structured Media*, Poznan University of Technology, Poznan, 312-326 (2002).
11. K. Wilmanski: Macroscopic modeling of porous and granular materials - microstructure, thermodynamics and some boundary-initial value problems, Keynote Lecture at CANCEM 2003, WIAS-Preprint No. 858 (2003).
12. K. Wilmanski, B. Albers: Acoustic waves in porous solid-fluid mixtures, in: *Dynamic Response of Granular and Porous Materials under Large and Catastrophic Deformations*, K. Hutter, N. Kirchner (eds.), Lecture Notes in Applied and Computational Mechanics, Vol.11, Springer, Berlin, 285-314 (2003).